Confinement and curvature effects as a tool for selectivity orientation in heterogeneous catalysis: Isomerisation of *n*-hexene over MCM-41-type catalysts

Nathalie Tanchoux, Stéphane Pariente, Philippe Trens*, François Fajula

*Institut Charles Gerhardt, UMR 5253 CNRS/ENSCM/UM2/UM1, Matériaux Avancés pour la Catalyse et la Santé (MACS),
Ecole Nationale Supérieure de Chimie, 8 rue de l'Ecole Normale, 34296 Montpellier Cedex 5, France*

ARTICLE INFO

ABSTRACT

In this paper, it is shown that confinement or curvature effects can significantly influence catalytic processes when using mesoporous catalysts. MCM-41-type materials have been prepared and carefully characterized to ensure that the only difference between these catalysts is the pore size. 1-Hexene used as reagent has been adsorbed in siliceous MCM-41 materials featuring identical pore sizes to determine the different sorption processes as a function of pressure. Catalysts with a high Si/Al ratio have been used for the isomerisation of 1-hexene into 2-hexene under different 1-hexene partial pressures corresponding to those of the different sorption regimes. It is demonstrated that confinement/curvature effects impact catalytic behaviour at two different levels: (i) different pore sizes result in different reaction and deactivation rates and (ii) different reagent partial pressures (or sorption regimes) for a given pore size lead to a striking inversion of selectivity between the *cis*- and *trans*-2-hexene isomers.

© 2008 Elsevier B.V. All rights reserved.

1. Introduction

Historically, confinement effects have been first studied using zeolites as model sorbents with the sorption of hydrocarbons, aromatics or water [1–4]. Models have been developed to understand their high efficiency for adsorbing any kind of species and curvature effects have been envisaged quite early to describe sorption properties of zeolites. Derouane has been one of the pioneers in this field with the concept of "nest-effect" developed in the late 80'. A striking evidence of this concept is the demonstration that up to 40% of the heat of adsorption of amines in the porosity of zeolites (MFI, MOR) could be assigned to confinement effects [4]. Following this concept, a rather similar type of approach allowed correlating the enthalpies of adsorption in the case of any sorbing system to geometric parameters related to both the zeolite and the sorbate species [5]. Improving the understanding of zeolites as sorbents, Derouane also suggested that zeolites could be envisaged as solid solvents so that the physicochemical properties of sorbed species could be driven by solvation effects [6]. Experimental studies confirmed this suggestion, for instance in the case of the measurable sorption of benzene in the ZSM-5 zeolite, despite the fact that benzene has a larger size as compared to the pore opening of the zeolite. Derouane completed his view on the physical state of molecules in

micropores, suggesting that these molecules could be in a pseudo-supercritical state, with intermediate physicochemical properties [7].

Mesoporous materials also allowed studying confinement effects. This was made possible by the existence of Vycor glasses, or more recently highly structured mesoporous materials such as MCM-41 or SBA-15. These materials were at the base of both experimental and theoretical studies devoted to the influence of various parameters such as particle or pore size onto physicochemical properties of fluids like phase transformations [8–16], diffusion [17,18], sorption [19–21] or catalytic properties [22]. In a recent paper, Goettmann and Sanchez highlighted strong relationship between confinement effects and heterogeneous catalysis [23], in the particular case of mesoporous materials.

They studied the catalytic activity of a rhodium complex anchored on mesoporous MCM-41-type silicas of various pore sizes in 1-hexene hydrogenation with different solvents. They could evidence a particular pore size leading to a maximum conversion of 1-hexene, without providing any molecular level explanation. They concluded that "confinement effects" should rule this catalytic reaction. By analogy with other systems they further proposed that energy exchanges at the adsorbed phase/bulk phase interface could play a major role in controlling the behaviour of a given phase.

The reaction chosen in this paper is the isomerisation of 1-hexene rather than its hydrogenation. The isomerisation of linear alkenes (1-butene, 1-pentene, 1-hexene, and 1-heptene) has already been widely studied in the past [24–26]. This reaction is

---

* Corresponding author. Tel.: +33 467 163 484; fax: +33 467 163 470.
  E-mail address: tchx@gmx.net (P. Trens).

catalysed by acidic catalysts and occurs through the formation of an intermediate carbocation resulting in the formation of *cis*- and *trans*-isomers of the starting material. The reason for that is quite simple: keeping the same physicochemical properties in the solvent phase, made of the reagent and products, is more straightforward if the products have properties similar to the reagent. This is precisely the case of 2-hexene as product, keeping in mind that the aim here is not to improve by any means this classical reaction, but more to take this reaction as a test to evidence confinement effects.

2. Experimental

2.1. Chemicals

1-Hexene used for this study has been provided by Aldrich (>99.0%). It was outgassed and stored over activated 3 Å molecular sieve prior to use as adsorbate or reactant.

2.2. Mesoporous solids preparation

The different mesoporous materials used in this work either as adsorbents (purely siliceous) or as catalysts (mildly acidic materials containing Al within their framework) were synthesized in the laboratory using hexadecyl trimethyl ammonium cations (namely 2.3-Al-MCM-41 and 2.5-MCM-41) and swelling agents as hexadecyl dimethyl amine (3.7-Al-MCM-41, 3.7-MCM-41, 4.4-MCM-41 and 4.6-Al-MCM-41) and trimethyl benzene (8.4-MCM-41 and 9.3-Al-MCM-41) in order to modulate the pore size [27]. The acidic mesoporous materials used for the catalytic tests were prepared by adding $NaAlO_2$ to the reaction medium. A very high Si/Al ratio

(Si/Al = 400) was used in order to confer a moderate acidity to the mesoporous materials sufficient to catalyze the chosen test reaction, while retaining textural properties as close as possible to the purely siliceous materials. Templates were removed by calcination in air flow (30 mL min^{-1}) at 773 K for 8 h [28].

2.3. Textural characterization

2.3.1. Nitrogen adsorption measurements

The materials were characterized by nitrogen adsorption at 77 K, using a Micromeritics ASAP 2010 automatic analyzer. Three typical nitrogen sorption isotherms are shown for the whole range of pore diameters in Fig. 1. For all materials, the nitrogen adsorption results in type IV sorption isotherms, typical of mesoporous materials. The sorption isotherms classically exhibit the different adsorption steps: first the monolayer–multilayer adsorption step; followed by a capillary condensation process, which steepness indicates a very narrow pore size distribution (Fig. 1). A flat saturation plateau obtained at higher equilibrium relative pressure indicates the small extent of external surface on which the adsorption process carries on. The textural properties of the materials are given in Table 1. The pore size distribution has been calculated according to the method developed by Broekhoff and de Boer [29,30] applied to the adsorption branch of the sorption isotherms, which takes into account the curvature of the pore section and has been proven to be more precise than other methods of pore size evaluation such as the 4 V/S method [31]. Specific surface areas were determined using the classical model developed by Brunauer, Emmett and Teller, taking 0.162 nm^2 as cross-sectional area for nitrogen [32]. The absence of micropores was checked by using the α_s comparing method.
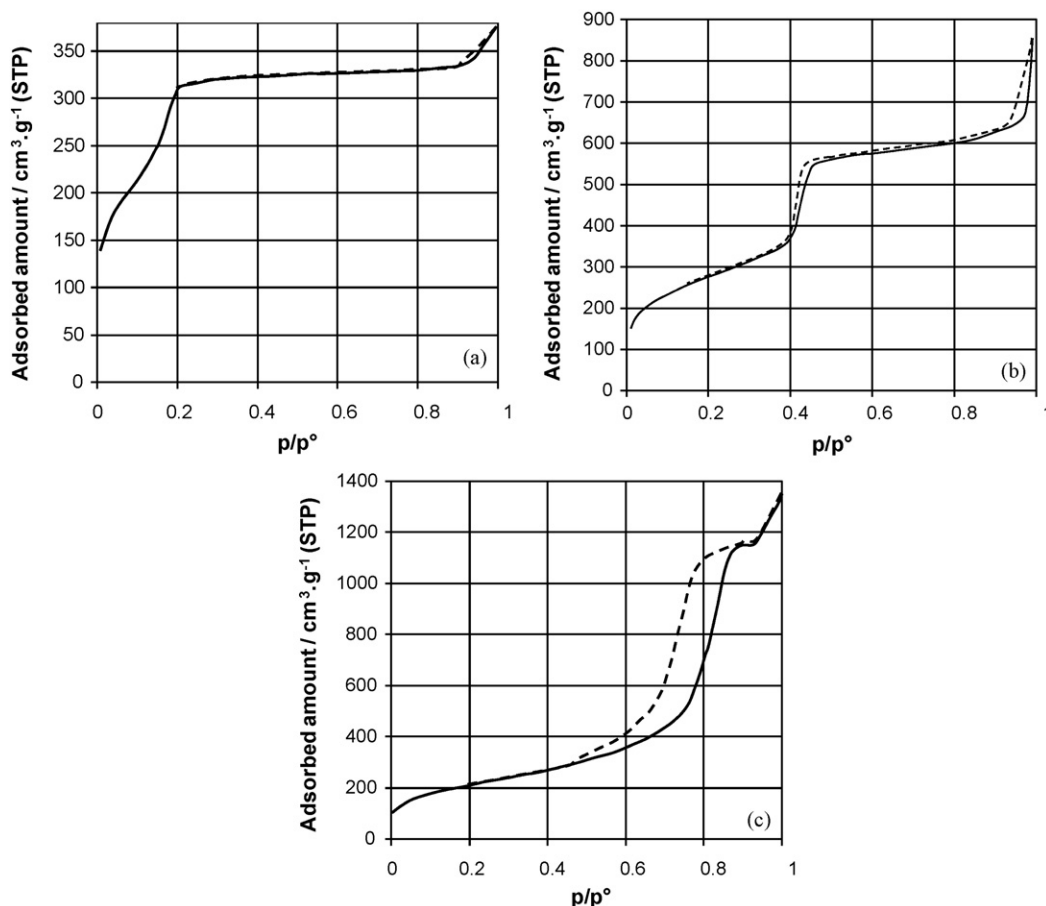

Fig. 1. Typical N_2 adsorption–desorption isotherms measured at 77 K for three Al-MCM-41 materials: (a) 2.3 nm; (b) 3.7 nm; and (c) 9.3 nm.

Table 1
Textural properties of the mesoporous materials.

Sample	Surface area ($m^2 g^{-1}$)	Pore diameter (nm)	Pore volume ($mL g^{-1}$)	Si/Al	Cell parameter (nm)
2.3 Al-MCM-41	–	2.3	0.52	400 ± 20	3.7
2.5 MCM-41	965	2.5	0.73	–	3.7
3.7 Al-MCM-41	981	3.7	0.96	400 ± 20	5.0
3.7 MCM-41	985	3.7	0.97	–	5.0
4.6 Al-MCM-41	861	4.6	0.77	400 ± 20	5.9
4.4 MCM-41	1180	4.4	1.11	–	5.7
9.3 Al-MCM-41	781	9.3	1.83	400 ± 20	14.2
8.4 MCM-41	924	8.4	1.99	–	12.2

2.3.2. X-ray diffraction measurements

Powder X-ray diffraction (XRD) spectra were obtained using a Siemens D5000 Diffractometer and monochromatic Cu Kα radiation. The materials with pore sizes up to 4.6 nm exhibited the XRD pattern typical of the *P6mm* structure of MCM-41-type materials, characterized by the [1 0 0] [1 1 0] and [2 1 0] reflections. The materials with pore sizes equal to 8.4 and 9.3 nm demonstrated a lower degree of long-range ordering, as it is generally observed. The lattice *a* parameters of the calcined materials are given in Table 1.

2.3.3. Characterization of the acidity

The acidity of the four samples containing aluminum was evidenced through IR measurements and thermodesorption of ammonia. The IR spectra were recorded using a Bruker IFS55 in the diffuse reflectance mode on the bare solids, in the presence of pyridine (strong adsorbed base) and CO (weak adsorbed base). They revealed the sole presence of isolated and geminal silanols groups with weak acid character. Strong acidic sites, associated with the presence of aluminium atoms in the framework, could not be detected with this technique, due to their very low concentration. The programmed thermodesorption (TPD) of ammonia performed on a homemade apparatus based on conductivity measurements, led to amounts of acid sites at the limit of detection of the method ($<0.05 \, mmol \, g^{-1}$). These results are similar for the four samples, which can then be considered as equivalent in terms of acidity, and are in line with the Si/Al ratio of 400 ± 20, determined by elemental analysis (SCA, Solaize, France).

2.4. Adsorption experiments

Sorption isotherms of 1-hexene over purely siliceous samples were determined using a homemade apparatus fully described elsewhere [33]. The adsorption apparatus is based on pressure measurements, the adsorption/desorption processes being followed by two capacitive pressure gauges (10 and 100 Torr). The whole apparatus is placed in a climatic chamber allowing a thermal stability better than 0.1 K from 250 K up to 350 K. The sample cell can be disconnected from the system so that the samples can be thermally treated at 523 K under vacuum (10^{-3} Torr) during 8 h between each experiment. Each experiment used ~150 mg of solid and the isotherms were determined for temperatures going from 293 K up to 343 K.

2.5. Catalytic experiments

The isomerisation of 1-hexene was investigated at 343 K in a homemade continuous fixed bed reactor, which has been fully described elsewhere [22]. The 1-hexene flow rate was maintained constant at $40 \, mL \, min^{-1}$, while the nitrogen flow rate ranged between 3.0 and $50 \, mL(STP) \, min^{-1}$ thus allowing a precise control of the 1-hexene partial pressure required to study its influence in the whole sorption regimes. A correlation between equilibrium relative pressures obtained for the adsorption isotherms and partial pressures established as described above seems reasonable since nitrogen does not adsorb onto aluminosilicate mesoporous materials at 343 K. Thus, as the only role of nitrogen is the elution of 1-hexene to reach different partial pressures, the adsorption isotherms can be used to determine the state of the pores for a particular partial pressure, that is submonolayer completion, mono-multilayer adsorption process or pores filled with sorbate.

On-line analysis of the gaseous effluents were performed by gas chromatography using a capillary column Chromopack Al_2O_3/KCl ($d_{int} = 0.53$ mm; $L = 50$ m) at 403 K. Besides the remaining unreacted substrate (1-hexene) and the main reaction products (*trans*-2-hexene and *cis*-2-hexene), the only by-products observed were (*cis* + *trans*)-3-hexene, 2-methyl-2-pentene and 2-methyl-1-pentene in amounts always lower than 5% of the total amount of products.

Preliminary catalytic tests were performed using purely siliceous MCM-41 materials as catalysts. No measurable conversion of 1-hexene could be observed. This point made clear, pure siliceous MCM-41 could be used for the determination of sorption isotherms of 1-hexene representative of the sorption isotherms that could have been obtained using (Si/Al = 400) MCM-41 catalysts.

3. Results and discussion

3.1. Sorption isotherms of 1-hexene

Sorption isotherms of 1-hexene have been determined on the purely siliceous materials featuring different pore sizes at temperatures going from 303 K to 343 K. This insures that no catalytic reaction takes place during sorption equilibria. The isotherms determined at 303 K for the whole range of materials used in this study are shown in Fig. 2. All the curves obtained are type IV isotherms, typical of mesoporous materials. The adsorption process in these materials is well known and can be described through several steps. At low relative pressure, the adsorption follows a
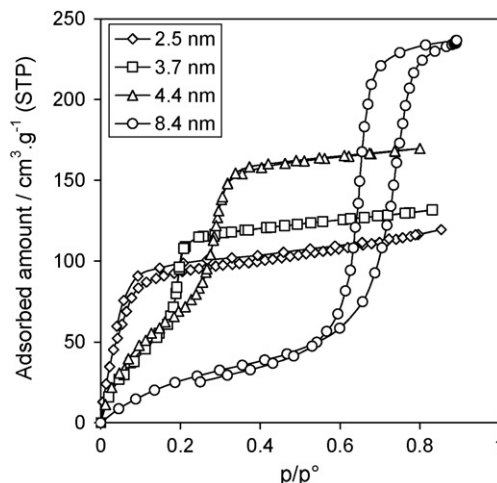

Fig. 2. Sorption isotherms of 1-hexene on different pore size materials at 303 K.
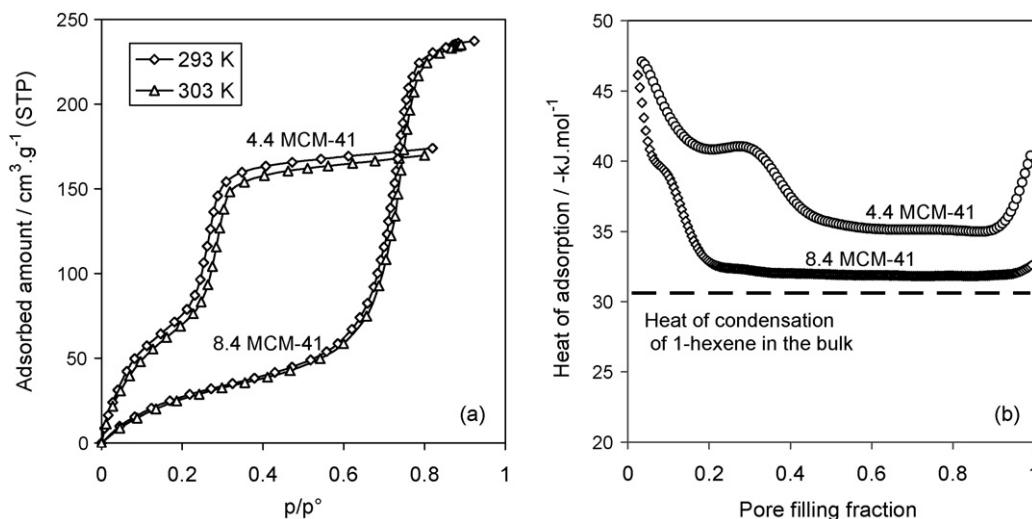
Fig. 3. (a) Sorption isotherms of 1-hexene on 4.4 MCM-41 and 8.4 MCM-41 at 293 K and 303 K and (b) corresponding heats of adsorption derived from the isotherms vs. pore filling fraction.

monolayer–multilayer adsorption mechanism, which is then followed by a capillary condensation process, characterized by a strong sorbate uptake, and finally adsorption takes place on the external surface. In our case, as it was already described elsewhere [34], the steep capillary condensation uptakes show the narrow distribution of pore size and the very flat plateaus are a proof of the small extent of external surface of our model materials. In the case of the 2.5 MCM-41 material, the 2.5 nm pore size is at the frontier of the microporous domain, thus exhibiting a hybrid type of isotherm, between type I and type IV. As shown in Fig. 2, the capillary condensation begins before the end of the monolayer completion, thus masking the knee that normally clearly appears before capillary condensation for mesoporous materials.

When comparing the different materials, and in accordance with other studies published in the literature, the increase of pore size or temperature (not shown here) shifts the capillary condensation uptakes towards higher relative pressures [35–39]. On the other hand, the effect of these two parameters on the hysteresis loop is opposed, as an increase of temperature (not shown here) for a given pore size leads to a narrowing, then disappearance of the loop, while an increase of pore size at a given temperature leads to the appearance and enlargement of this loop. It should also be noted that the capillary condensation occurs at low relative pressures – between 0.05 and 0.3 – for the three materials with the smallest pore size (2.5 MCM-41, 3.7 MCM-41, and 4.4 MCM-41), while it occurs for relative pressures as high as 0.6–0.8 for the 8.4 MCM-41 material. This point should be of importance as the catalytic process must depend on the state of the reactant within the pores, thus directly related to the temperature, pore size and filling state of the pores used for the catalytic tests.

3.2. Isosteric heats of adsorption

The heats of adsorption of 1-hexene on MCM-41 materials can be derived from the sorption isotherms through the well-known isosteric method. These heats of adsorption can be calculated from a set of sorption isotherms using an equation derived from the Clausius–Clapeyron equation (Eq. (1)):

$$\Delta_{ads}\dot{h} = -RT^2 \times \left[\frac{\partial(\ln\ p)}{\partial T}\right]_n \tag{1}$$

This method, which has already been described in detail elsewhere, can be applied under several conditions: (i) the temperature

range in which the different isotherms have been determined must not be too large; (ii) the structure of the adsorbed phase is supposed to be unchanged throughout the considered temperature range; and (iii) for a fixed adsorbed amount, the structure of the adsorbed phase must be identical at the different temperatures considered [38].

The results obtained for the 4.4 MCM-41 and 8.4 MCM-41 materials are shown in Fig. 3. The evolution of isosteric heats of adsorption has been represented with increasing pore filling fraction, which is the normalization of the adsorbed amount to the amount adsorbed at the saturation plateau. This representation has been chosen to facilitate the comparison between the different materials as the adsorbed amounts are very different from a solid to another (Fig. 3a). In the case of the 8.4 MCM-41 material the adsorbed amount at saturation has been estimated by considering that the density of 1-hexene is constant during pore filling, and by using the total pore volume calculated from nitrogen adsorption experiments.

The curves obtained (Fig. 3b) clearly exhibit the different steps of the adsorption process. At low pore filling fractions (up to 0.1 and 0.3, respectively, for the 4.4 MCM-41 and 8.4 MCM-41 materials) the monolayer–multilayer adsorption process takes place, followed by the capillary condensation characterized by constant heats of adsorption during the whole process thus indicating true first-order phase transitions, and finally the residual adsorption on the external surface of the materials leads to a divergence of the curves. The affinity of 1-hexene for the silica surface allows to clearly distinguish the different steps of the adsorption processes as can be seen in Fig. 3b. The results obtained in the case of the 2.5 MCM-41 materials (not shown here) exhibit a bell-shaped curve, thus confirming that this material is at the limit between the microporous and mesoporous domains, and in this case, the isosteric method should not be applied.

The influence of pore size is also remarkable as the isosteric heat of condensation (during capillary condensation process) is found higher than the heat of condensation of 1-hexene in the bulk ($-30.6\ kJ\ mol^{-1}$) in all cases. Moreover, these enthalpic excesses increase when the pore size of the material decrease, even in the case of the 2.5 MCM-41, where the whole curve is largely above the curve obtained for the 4.4 MCM-41 material (the enthalpic excess in this case is roughly 20 kJ mol^{-1}). These results are consistent with studies already published in the literature [40,41] and provide a quantitative insight into the influence of the surface curvature of the MCM-41 hosts on the adsorption process of 1-hexene.
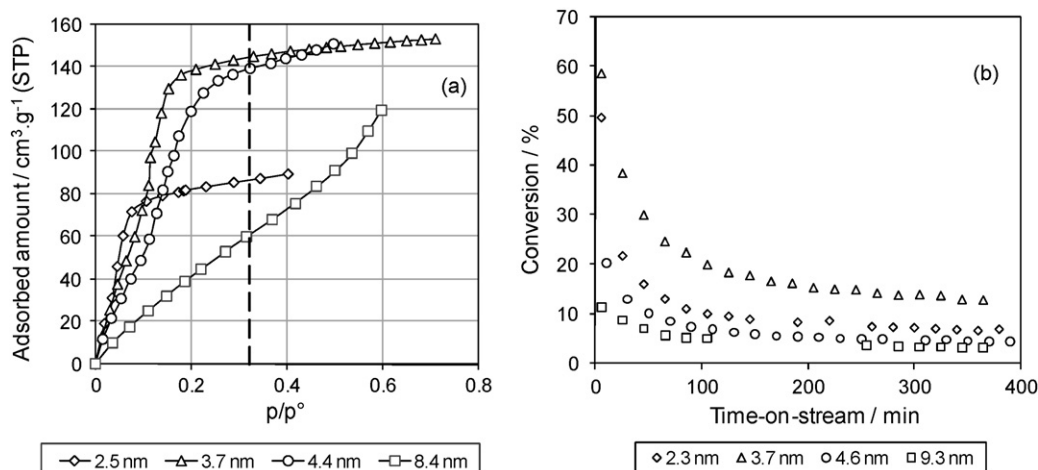
Fig. 4. (a) Sorption isotherms of 1-hexene on different purely siliceous materials at 343 K, the dash line corresponds to the relative pressure used for the catalytic tests showed in (b) and (b) conversion vs. time-on-stream for the isomerisation of 1-hexene over Al-MCM-41 catalysts of different pore sizes for the same partial pressure $p/p° = 0.32$.

3.3. Catalytic results

The chosen model reaction is the catalytic isomerisation of 1-hexene into *cis*- and *trans*-2-hexene over mildly acidic Al-MCM-41 catalysts, which presents several advantages: (i) this reaction is monomolecular; (ii) it has been performed without any solvent (the reactant playing the role of the solvent under certain pore filling conditions, see below), thus eliminating a parameter which would have rendered the system more complex; and (iii) the reaction temperature (343 K) allows the determination of sorption isotherms at the same temperature as the catalytic tests, which allows to fix precisely the pore filling conditions during the reaction. The reaction has been performed at 343 K on Al-MCM-41 catalysts with pore sizes ranging from 2.3 nm to 9.3 nm, with Si/Al ratios of 400. The high ratio has been chosen for several reasons: (i) the goal of this study is clearly not to obtain the highest possible conversions, but to precisely control the reactivity under identical conditions for all the catalysts with varying pore sizes and (ii) the amount of aluminium introduced in the catalysts is sufficiently low to consider that these catalysts are "identical" to their purely siliceous counterparts, meaning that the sorption isotherms determined for these materials can be used to set the pore filling conditions during the catalytic tests.

A series of sorption isotherms of 1-hexene on the purely siliceous MCM-41 materials has been determined at 343 K, in order to deduce the pore filling conditions at which the catalytic tests must be

performed (Fig. 4a). Each catalyst was then tested for different 1-hexene partial pressures, each partial pressure corresponding to a single test, using fresh catalyst for each test. It must be recalled that purely siliceous materials were tested and proved totally inactive. The pore filling conditions within the catalytic reactor being fixed by nitrogen and 1-hexene flow rates, the range of attainable partial pressures – which correspond to the relative pressures of the isotherms (see Section 2) – goes from 0.13 to 0.6 due to these technical limitations. This means that even at the lowest partial pressure (0.13), the pores of the two smallest pore catalysts (2.3 Al-MCM-41 and 3.7 Al-MCM-41) are already filled, while at the highest partial pressure (0.6) the adsorption process is barely at the end of the monolayer completion for the largest pore catalyst (9.3 Al-MCM-41). Consequently, the only catalyst for which the influence of pore filling can be thoroughly investigated is the 4.6 Al-MCM-41 catalyst, as the experimental conditions allow to go through the whole adsorption process.

For the sake of clarity, the conversion versus time-on-stream curves are presented here for different catalysts but for a single partial pressure (0.32) (Fig. 4b). The same typical curves were obtained for all the catalysts and all the partial pressures tested. All curves indicate high initial activities with a fast deactivation, and a stabilization for long times-on-stream. It can be noted in all cases that the initial activity is inversely proportional to the pore size and the smaller the pore size the faster the deactivation. Such a correlation between overall activity and deactivation rate is commonly
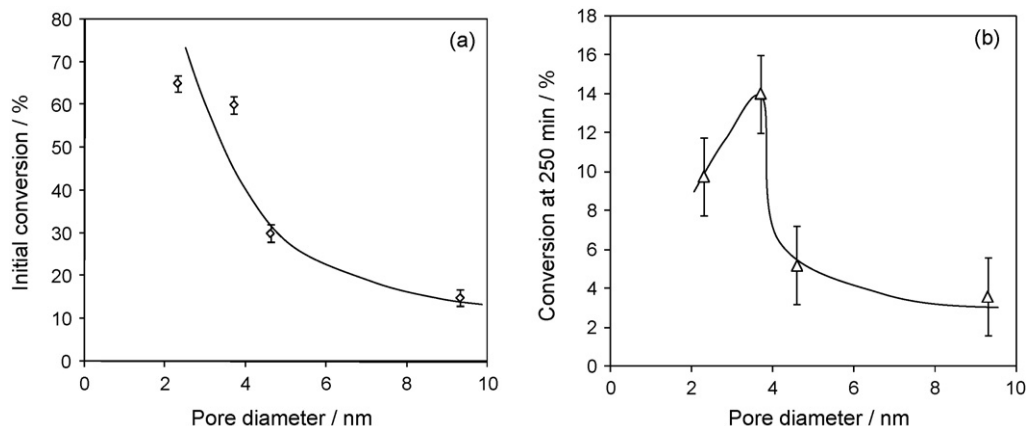

Fig. 5. (a) Initial conversion as a function of pore diameter for the isomerisation of 1-hexene at 343 K over Al-MCM-41 catalysts and (b) conversion at 250 min as a function of pore diameter for the isomerisation of 1-hexene at 343 K over Al-MCM-41 catalysts.
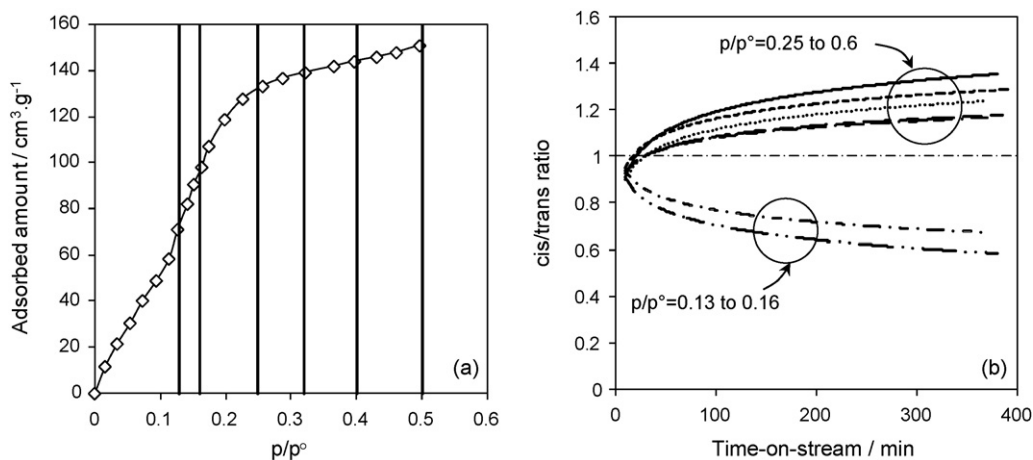
Fig. 6. (a) Adsorption isotherm of the 4.4 MCM-41 purely siliceous material at 343 K, each line corresponding to a pore filling condition tested in the catalytic test and (b) influence of the pore filling conditions on the selectivity of the reaction at 343 K.

observed in the case of acidic catalysts. The poisoning of the sites indeed results from the accumulation of heavy residues produced as by-products via mechanism not different from those of the target reaction. The results clearly evidence therefore the influence of pore size on the catalytic activity, either for short times-on-stream, or after the deactivation period when the activity is stabilized.

In order to assess more clearly the influence of pore size on activity, the evolution of the initial conversions and of the conversions after 250 min on stream have been represented in Fig. 5 as a function of pore diameter. For each pore size, the value represented corresponds to the mean value of all the partial pressures tested, the error bar corresponding to the distribution of experimental conversions obtained. The chart representing the initial conversion versus pore diameter confirms the direct influence of pore size on the catalytic activity. It shows a decrease of initial activity with the increase of pore size, the catalyst exhibiting the highest initial activity being the 2.3 Al-MCM-41 sample. As the four catalysts tested are chemically identical, differences in acidities or surface state cannot be invoked to explain these results.

The conversion levels achieved after 250 min on stream reveal a bell-shaped curve which could apparently contradict the results obtained for short times-on-stream. However, the catalyst with the smallest pore sizes (2.3 Al-MCM-41) is the most active catalyst as well as the catalyst that deactivated the fastest among the series. The most plausible explanation could be that the diffusion within the pores of the 2.3 Al-MCM-41 catalyst, at the frontier of the microporous domain, is severely limited, due to the formation of heavy products.

As already discussed in a previous work [22], the effect of pore size on catalytic activity can be qualitatively and quantitatively accounted for by the Nest effect model developed by Derouane in the case of zeolite catalyzed reactions [6]. Derouane indeed clearly demonstrated the direct relationship between catalytic activity and adsorption enthalpies of the reactant within the pores of the catalyst. The enthalpic excesses found in the case of 1-hexene adsorption over MCM-41 materials are inversely proportional to the pore size. They can be associated with catalytic activity as the highest enthalpic excess (2.5 MCM-41) corresponds to the highest catalytic activity, while the lowest enthalpic excess (8.4 MCM-41) also corresponds to the lowest catalytic activity either at short or long times-on-stream (cf. Fig. 5).

Because of the identical chemical nature of the catalysts, this result constitutes a clear evidence of the relationship between catalytic activity and surface curvature, or so-called "confinement effects" in the case of mesoporous materials.

Conversion, however, is not the only indicator measuring the influence of pore size or pore filling on the catalytic process. Selectivity could as well be influenced by any of these parameters.

A most striking result was obtained when plotting the evolution of the cis-2-hexene/trans-2-hexene ratio versus time-on-stream for the different partial pressures (and degree of pore filling) tested for the 3.7 Al-MCM-41 and 4.6 Al-MCM-41 catalysts. For technical reasons the same series of experiments could not be performed for the 2.3 Al-MCM-41 and 9.3 Al-MCM-41 catalysts. With the former, the pores were already totally filled at the lower pressure achievable, while in the case of the later the highest partial pressure attainable with our set-up corresponded to only the end of monolayer completion of the adsorption process.

As shown in Fig. 6 related to the experiments performed over the 4.6 Al-MCM-41 catalyst, an inversion of selectivity clearly occurs, particularly noticeable after some time on stream, when the strongest acid sites have been poisoned. On the fresh catalyst, under all pore filling conditions, at a conversion level of $22 \pm 3\%$, all runs led to a cis/trans ratio equal to 0.9. By contrast, after a few minutes on stream the reactions carried out before and during the capillary condensation ($p/p° = 0.13$ and 0.16) lead to a majority of trans isomer (thermodynamically favoured product) while the experiments carried out after the capillary condensation ($p/p° = 0.25$–0.6) lead to a majority of cis isomer (kinetically favoured product). Because deactivation results in a decrease in conversion, the selectivity data have been reported as a function of conversion in Fig. 7a–c. As expected, this representation confirms that the different degrees of pore filling lead to different catalytic systems and accordingly to different kinetic regimes: at low partial pressures, the system is characterized by an adsorbed phase/vapour phase equilibrium, with a strong enthalpic excess due to the occurrence of an interface [42,43], while at the high partial pressures, when the pores are saturated with the liquid reagent, the reaction proceeds in the presence of a solvent. These two different situations definitely impact adsorption–desorption constants of the reactant and products and as a consequence the overall free energy profile of the isomerisation process changes. The cis-2-hexene is indeed known to be slightly more basic than the trans isomer, thus leading to a strongest adsorption on the surface of the catalyst at low partial pressure, which could favour the formation of trans product. In the case of higher partial pressures, the complete filling of the pores and a higher 1-hexene partial pressure could force the desorption of the cis isomer, and lead to the observed inversion of selectivity. This hypothesis would be in line with the conclusions of a recent study on confinements effects in heterogeneous catalysis which stated that confinement effects could promote selective adsorption [44].
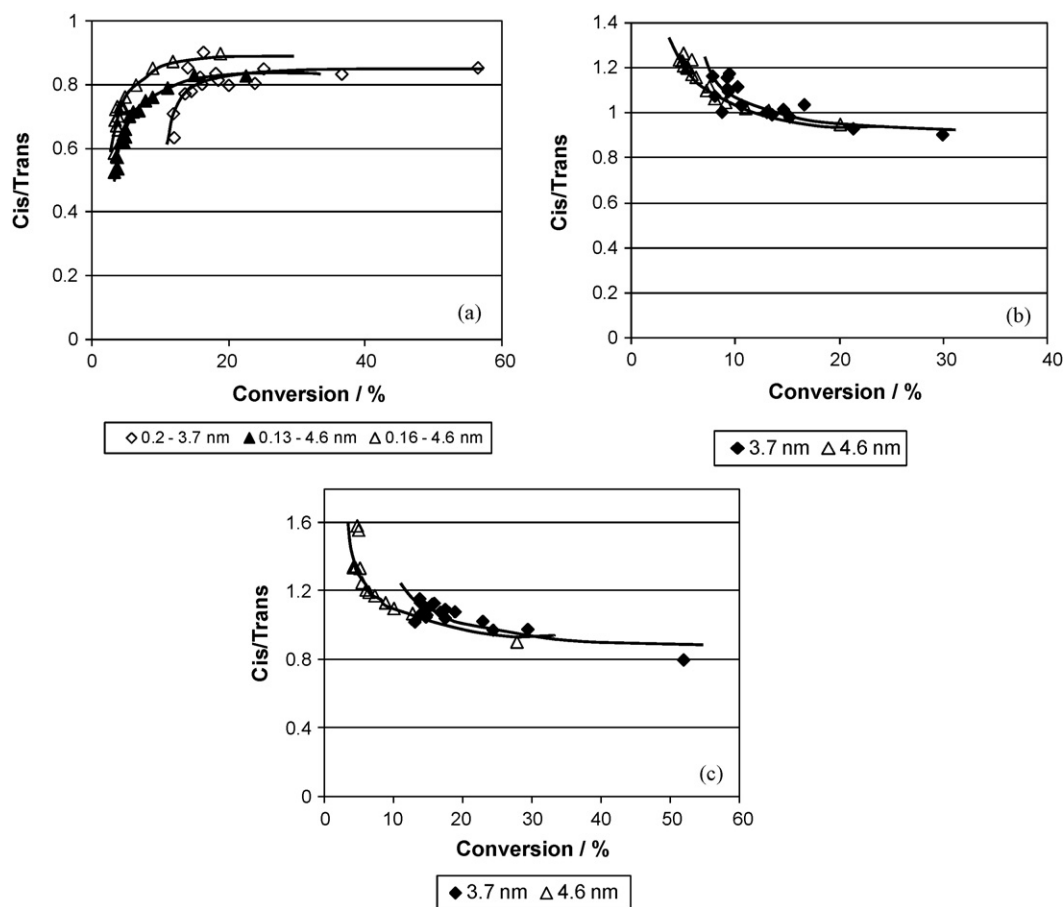
Fig. 7. Influence of the conversion on the selectivity of the isomerisation (a) at low pore filling conditions ($p_{hexene}/(p_{hexene} + p_{nitrogen}) = 0.13$, 0.16 and 0.2 and (b) at $p_{hexene}/(p_{hexene} + p_{nitrogen}) = 0.25$ and (c) at completely filled pores ($p_{hexene}/(p_{hexene} + p_{nitrogen}) = 0.6$) for 3.7 Al-MCM-41 and 4.6 Al-MCM-41 catalysts.

4. Conclusion

In this paper, it is shown that confinement and/or curvature effects in mesoporous materials can affect selectivity in heterogeneous catalysis. These effects could be demonstrated by using MCM-41-type materials prepared with a wide range of pores sizes and carefully characterized, ensuring that the only difference between these materials is pore size. 1-Hexene used as reagent has been adsorbed in siliceous MCM-41 materials in the temperature range relevant to catalytic studies to allow the determination of the different sorption processes as a function of pressure. Catalysts with a high Si/Al ratio have been used for the isomerisation of 1-hexene into 2-hexene with different 1-hexene partial pressures corresponding to those of the different sorption regimes. The effect of the confinement is apparent at two levels: (i) different pore sizes result in different reaction and deactivation rates and (ii) different reagent partial pressures (or sorption regimes) for a given pore size allow a striking inversion of selectivity between the *cis*- and the *trans*-2-hexene isomers. It is assumed that the latter effect results from a change in the solvent properties of the *n*-hexene reagent which, in turn, affect the sorption characteristics of the products. Such a phenomenon could constitute a new tool for the orientation of the selectivity in catalytic processes involving low energy barriers between competing paths.

References

[1] A. Corma, Chem. Rev. 97 (1997) 2373.
[2] F. Marquez, H. Garcia, E. Palomares, L. Fernandez, A. Corma, J. Am. Chem. Soc. 122 (2000) 6520.
[3] N. Floquet, J.P. Coulomb, N. Dufau, G. André, J. Phys. Chem. B 108 (2004) 13107.
[4] E.G. Derouane, J.M. André, A.A. Lucas, J. Catal. 110 (1988) 58.
[5] Z. Blum, S.T. Hyde, B.W. Ninham, J. Phys. Chem. 97 (1993) 661.
[6] E.G. Derouane, J. Mol. Catal. A: Chem. 134 (1998) 29.
[7] E.G. Derouane, Micropor. Mesopor. Mater. 104 (2007) 46–51.
[8] C. Alba-Simionesco, B. Coasne, G. Dosseh, G. Dudziak, K. Gubbins, R. Radhakrishnan, M. Sliwinska-Bartkowiak, J. Phys. Condens. Matter 18 (2006) R15.
[9] E. Roduner, Chem. Soc. Rev. 35 (2006) 583.
[10] L.D. Gelb, K. Gubbins, R. Radhakrishnan, M. Sliwinska-Bartkowiak, Rep. Prog. Phys. 62 (1999) 1573.
[11] M. Brun, A. Lallemand, J.F. Quinson, C. Eyraud, Thermochim. Acta 21 (1977) 59.
[12] N. Tanchoux, P. Trens, D. Maldonado, F. Di Renzo, F. Fajula, Colloid Surf. A 246 (2004) 1.
[13] R. Zangi, J. Phys. Condens. Matter 16 (2004) S5371.
[14] S. Sklari, H. Rahiala, V. Stathopoulos, J. Rosenholm, P. Pomonis, Micropor. Mesopor. Mater. 49 (2001) 1.
[15] N. Floquet, J.P. Coulomb, J.P. Bellat, J.M. Simon, G. Weber, G. André, J. Phys. Chem. C 111 (2007) 18182.
[16] N. Floquet, J.P. Coulomb, N. Dufau, G. Andre, R. Kahn, Adsorption 11 (2005) 139.
[17] D. Plant, H. Jobic, P. Llewellyn, G. Maurin, Adsorption 13 (2007) 209.
[18] J.P. Korb, L. Malier, F. Cros, S. Xu, J. Jonas, Phys. Rev. Lett. 77 (1996) 2312.
[19] P. Trens, N. Tanchoux, A. Galarneau, F. Fajula, J. Phys. Chem. B 109 (2005) 16415.
[20] K. Morishige, M. Shikimi, J. Chem. Phys. 108 (1998) 7821.
[21] W.D. Machin, Langmuir 10 (1994) 1235.
[22] S. Pariente, P. Trens, F. Fajula, F. Di Renzo, N. Tanchoux, Appl. Catal. A: Gen. 307 (2006) 51.
[23] F. Goettmann, C. Sanchez, J. Mater. Chem. 17 (2007) 24.
[24] J. Manassen, S. Khalif, J. Catal. 7 (1967) 110.

[25] T. Uematsu, K. Tsukada, M. Fujishima, H. Hashimoto, J. Catal. 32 (1974) 369.
[26] P.M. Slomkiewicz, Appl. Catal. A: Gen. 301 (2006) 232.
[27] A. Sayari, Y. Yang, M. Kruk, M. Jaroniec, J. Phys. Chem. B 103 (1999) 3651.
[28] K. Hanna, I. Beurroies, R. Denoyel, D. Desplantier-Giscard, A. Galarneau, F. Di Renzo, J. Colloid Interf. Sci. 252 (2002) 276.
[29] J.C.P. Broekhoff, J.H. de Boer, J. Catal. 9 (1967) 8.
[30] J.C.P. Broekhoff, J.H. de Boer, J. Catal. 9 (1967) 15.
[31] A. Galarneau, D. Desplantier, R. Dutartre, F. Di Renzo, Micropor. Mesopor. Mater. 27 (1999) 297.
[32] S. Brunauer, P.H. Emmett, E. Teller, J. Am. Chem. Soc. 60 (1938) 309.
[33] N. Tanchoux, P. Trens, D. Maldonado, F. Di Renzo, F. Fajula, Colloid Surf. 246 (2004) 1.
[34] P. Trens, N. Tanchoux, P.M. Papineschi, D. Maldonado, F. Di Renzo, F. Fajula, Micropor. Mesopor. Mater. 86 (2005) 354.
[35] K. Morishige, H. Fujii, M. Uga, D. Kinukawa, Langmuir 13 (1997) 3494.
[36] S. Groß, G.H. Findenegg, Ber. Bunsenges. Phys. Chem. 101 (1997) 1726.
[37] P.C. Ball, R. Evans, Langmuir 5 (1989) 714.
[38] P.I. Ravikovitch, D. Wei, W.T. Chueh, G.L. Haller, A.V. Neimark, J. Phys. Chem. B 101 (1997) 3671.
[39] R. Pellenq, B. Rousseau, P.E. Levitz, Phys. Chem. Chem. Phys. 3 (2001) 1207.
[40] K.S.W. Sing, D.H. Everett, R.A.W. Haul, L. Moscou, R.A. Pierotti, J. Rouquerol, T. Siemieniewska, Pure Appl. Chem. 57 (1985) 603.
[41] A.V. Neimark, P.I. Ravikovitch, M. Grun, F. Schuth, K.K. Unger, J. Colloid Interf. Sci. 207 (1998) 159.
[42] P. Trens, N. Tanchoux, A. Galarneau, D. Brunel, B. Fubini, E. Garrone, F. Fajula, F. Di Renzo, Langmuir 21 (2005) 8560.
[43] P. Trens, N. Tanchoux, D. Maldonado, A. Galarneau, F. Di Renzo, F. Fajula, New J. Chem. 28 (2004) 874.
[44] E.E. Santiso, A.M. George, C.H. Turner, M.K. Kostov, K.E. Gubbins, M. Buongiorno-Nardelli, M. Sliwinska-Bartkowia, Appl. Surf. Sci. 252 (2005) 766.